JOMH
Journal of Men's Health

ORIGINAL RESEARCH

Stratification of risk based on immune signatures and prediction of the efficacy of immune checkpoint inhibitors in prostate cancer

Yidan Sun[1,†], Xinyu Yang[2,†], Shiqi Ren[3,†], Zhichao Lu[3], Zongheng Liu[3], Fanming Kong[1], Ziheng Wang[3,4],*, Yang Yang[5],*

[1]Department of Oncology, First Teaching Hospital of Tianjin University of Traditional Chinese Medicine, 300380 Tianjin, China
[2]Medical School of Nantong University, 226019 Nantong, Jiangsu, China
[3]Department of Clinical Biobank & Institute of Oncology, Affiliated Hospital of Nantong University, Medical School of Nantong University, 226001 Nantong, Jiangsu, China
[4]Centre for Precision Medicine Research and Training, Faculty of Health Sciences, University of Macau, 999078 Macau SAR, China
[5]Department of Trauma Center, Affiliated Hospital of Nantong University, 226001 Nantong, Jiangsu, China

*Correspondence
wang.ziheng@connect.um.edu.mo
(Ziheng Wang);
yangyang286228@ntu.edu.cn
(Yang Yang)

† These authors contributed equally.

Abstract

Prostate adenocarcinoma (PRAD) is a major threat to male health worldwide with a high mortality rate. New therapeutic strategies for the treatment of this malignant disease are of tremendous significance. Much attention has been paid to the involvement of immune cells in the prevention and treatment of cancer as well as how their regulatory systems contribute to effective cancer treatment. In this study, we constructed prognostic immune profiles based on The Cancer Genome Atlas (TCGA)-PRAD data sets and tested their predictive power on total and internal data sets. Then, we looked at how the lymphocyte of tumor invasion varied between the high-risk group and the low-risk group. Five immune-related genes made up the immune marker, which was an independent predictive factor in patients with PRAD. Patients in the low-risk score group had a higher rate of overall survival and a stronger infiltration of immune cells in the tumor microenvironment, which was highly related to clinical outcomes but required prospective validation.

Keywords

Prostate cancer; Tumor immune microenvironment; Immune checkpoint inhibitor; Immunotherapy; Prognostic model

1. Introduction

Prostate adenocarcinoma (PRAD) is a leading contributor to deaths in men globally [1]. In order to effectively treat this cancer, new therapeutic approaches are crucial [2]. Much focus has been paid to the involvement of immune cells in cancer treatment and prevention, as well as how their regulatory mechanisms provide effective cancer therapy. At present, Immunotherapy is a hot spot in clinical tumor therapy. A large number of clinical studies or basic experiments have proved that immune checkpoint inhibitors (ICIs) can play a wonderful role in tumor therapy [2]. Nevertheless, only a small proportion of cancer patients can benefit from ICIs, and the overall response rate is low [1]. In colorectal, ovarian and hepatocellular carcinoma, several immune-related genes (IRGs) have been identified as prognostic biomarkers. These genes have been linked to immune cells and relevant molecular mechanisms in the tumor microenvironment, and to some extent, they reflect the status of the immune response in the tumor microenvironment [3]. More recently, using transcriptome sequencing data, computer algorithms like Tumor Immune Estimation Resource (TIMER) [4] and CIBERSORT have made

it possible to determine the immune spectrum of cancer. The effect of immunotherapy is revealed by the immune landscape of cancer, which is also highly linked to patient prognoses. It is important to develop a comprehensive immune spectrum model to evaluate the immune-related efficacy of therapies. Few studies have conducted immune profiling and investigated IRGs for their predictive significance in PRAD. In this work, we developed an immune marker based on IRGs, and we looked at how it related to clinic-pathological characteristics and clinical outcomes in PRAD patients [5]. In addition, we investigated the molecular functions, cellular components and possible pathways of Different expressed immune-related genes (DEIRGs) enrichment in the prediction model by molecular enrichment analysis.

2. Materials and methods

2.1 Differentially expressed IRGs

All original data were obtained from the TCGA database. We examined the differentially expressed genes between PRAD and corresponding normal tissues to screen out IRGs involved in oncogenesis. The abnormally expressed genes were iden-

tified using the software edgeR (version 4.0.0, John Chambers and colleagues, Auckland, New Zealand) (https://www.r-project.org/), as described previously (adjusted p value < 0.05 and $|\log2 \text{ (fold change)}| > 1$). The intersection between differentially expressed genes and the IRGs was termed differentially expressed IRGs.

2.2 Pathway and functional enrichment analyses

We carried out Pathway and functional enrichment analyses to investigate the biological significance of these differentially expressed IRGs. Kyoto Encyclopedia of Genes and Genomes (KEGG) [6] and Gene Ontology (GO) [7] enrichment analyses were carried out. Terms and pathways were regarded as significantly enriched objects if their false discovery rate was less than 0.05. The package ggplot2 was used to carry out the visualization. Pathway illustrations were generated using the "pathview" R package.

2.3 Constructing an IRGs-related immune signature for PRAD

We identified immune genes associated with prognosis. To verify their robustness and predictive ability, we developed a prognostic risk model. We first screened for immune-related genes with prognostic significance by univariate Cox proportional hazards regression analysis. Genes with a p-value of less than 0.05 were examined by the glmnet software using the minimum absolute contraction and selection operator (Lasso) to prevent over-fitting [8]. After screening by the Lasso model, a multivariate Cox proportional hazards model was employed to develop the immune-related risk model as follows: risk score = Gene A level × coefficient a + gene B level × coefficient B + gene C level × coefficient C + ... + gene N level × coefficient N. The prognosis for PRAD patients is represented by the risk score in the model, where the lower the risk score, the better the prognosis. The patients were classified into high-risk and low-risk groups using the median risk score as the cut-off value. With log-rank p-value < 0.05 considered statistically significant (for packet survival and investigator), predictive ability was calculated using Kaplan-Meier survival curves. Using a time-dependent receiver operating characteristic curve (ROC), the prediction ability of this immune signature was evaluated [2, 9, 10].

2.4 Calculating the ratio of tumor-infiltrating immune cells

By using a deconvolution technique, CIBERSORT could determine the ratios of infiltrated immune cells from tissue transcriptional profiles. We computed the ratios of 22 types of tumor-infiltrating immune cells using the TCGA-PRAD transcriptional profiles and the CIBERSORT R script [11, 12].

2.5 Statistical analysis

Chi-square and Student's t-tests were conducted to examine differences among variables. The effects of multiple clinic-pathological characteristics along with the immune signature on patients' survival were evaluated using univariate and multivariate cox regression analyses [13]. Using R software programming language (version 0.0.0). Statistical analysis was carried out. The package "pheatmap" was used to create the heat maps. Statistical significance was defined as p-value < 0.05.

2.6 Quantitative reverse transcription-polymerase chain reaction (qRT-PCR)

The specific experimental steps are as described in the previous paper [14]. In brief, total RNA was extracted from normal tissue and tumor tissue from PRAD patients using TRIzol (15596026, Thermo Fisher Scientific, Waltham, MA, USA). Quantitative reverse transcription-polymerase chain reaction (qRT-PCR) was conducted on the obtained RNA from each sample (2 μg) with FastStart Universal SYBR® Green Master (4913914001, Roche, Basel, Switzerland., USA) on a Q5 PCR System (Roche, USA). The primers were showed in Table 1.

3. Results

3.1 Identification of prostate cancer prognosis-related differentially expressed genes

We first classified the prostate cancer samples in the TCGA database as "Alive" and "Dead" according to patients' overall survival profiles. After adjusting the cut-off value adjusted p value < 0.05 and $|\log2 \text{ (fold change)}| > 1$). Then, 1309 Differentially expressed genes were screened. At the same time, 2489 immune-related genes with an "Immune" correlation score greater than 2 were screened from the GeneCards database. After crossing, 18 immunologically related prognostic differentially expressed genes were obtained.

3.2 The prognosis of PRAD patients can be predicted by the five-gene immune signature

To evaluate the predictive significance of the chosen 18 differentially expressed IRGs and to avoid over-fitting, we further performed a LASSO analysis in which five of the 18 genes were predictors of patient outcome (Fig. 1A,B). We ranked patients' risk scores and outlined their distribution (Fig. 1C Top). A dot plot (Fig. 1C Middle) was used to display the risk scores, survival status and overall survival of the patients. The heat map displays the five IRGs' expression patterns in patients with varying risk scores. In the low-risk group, Insulin Like Growth Factor 1 (IGF1) and Opioid Receptor Kappa 1 (OPRK1) were expressed at high levels, whereas in the high-risk group, Anti-Mullerian Hormone (AMH), Defensin Alpha 5 (DEFA5) and Serum Amyloid A1 (SAA1) were expressed at high levels. The predictive ability of this immune signature was further verified. Prostate cancer patients were classified into high-risk and low-risk groups (categories). Those with low-risk scores had longer Overall survival (OS) duration, according to the survival analysis ($p = 0.004$) (Fig. 1D). Moreover, this immune signature's area under the curve (AUC) value was 0.875 (Confidence interval

TABLE 1. Forward and reverse primer on gene signatures of prognostic models.

Gene	Forward primer (5′-3′)	Reverse primer (5′-3′)
AMH	ACTCATCCCCGAGACCTACC	CGATGCTTGGGGTCCGAATA
DEFA5	GTCTGGGGAAGACAACCAGG	GTAGAGGCGGCCACTGATTT
IGF1	AGAGCCTGCGCAATGGAATA	ACCCTGTGGGCTTGTTGAAA
OPRK1	TCGTGATCATCCGATACACAAAGA	CGATCTTTCTCTCGGGAGCC
SAA1	CAGATCAGGTGAGGAGCACAC	CATAGTTCCCCCGAGCATGG
GAPDH	AATGGGCAGCCGTTAGGAAA	GCCCAATACGACCAAATCAGAG

AMH: Anti-Mullerian Hormone; DEFA5: Defensin Alpha 5; IGF1: Insulin Like Growth Factor 1; OPRK1: Opioid Receptor Kappa 1; SAA1: Serum Amyloid A1; GAPDH: Glyceraldehyde-3-Phosphate Dehydrogenase.

(CI): 0.796–0.953) (Fig. 1E). Time-dependent ROC curves at 1-year, 3-year and 5-year durations (AUC = 1.000, 0.891 and 0.912, respectively) are also displayed (Fig. 1F).

3.3 The tumor immune microenvironment and the 5-IRG signature

To generate histograms displaying the proportion of 22 immune cells infiltrating in tissue samples from the PRAD patients, we computed the proportion of 22 immune cell types in each PRAD sample using the CIBERSORT method (Fig. 2A,B). The proportion of immune cells that differed between the groups with high and low-risk scores was compared. The percentage of B cells, Eosinophils, Macrophages, mast cells, Neutrophils, NK (Natural killing cell) CD56 (Neural Cell Adhesion Molecule 1) bright cells, NK cells Tgd, PDC (plasmacytoid dendritic cell), Th1 cells and T helper cells differed remarkably (Fig. 2C) [15].

We compared the expression differences of prognostic DEirgs in TCGA-PRAC, with only AMH being significantly overexpressed in the tumor (Fig. 3A) while having the same expression differences in paired samples of tumor tissue (Fig. 3B). The expression of the five genes was significantly different and were demonstrated using a between-group differential gene volcano map (Fig. 3C) and a sequence map (Fig. 3D) based on patient survival status. Subsequently, both univariate and multivariate Cox regression analyses were carried out to investigate the prognostic value of model DEIRGs (Fig. 3E,F & Table 2).

3.4 Relationship between survival prognosis and 5-gene expression difference in prostate cancer patients

We explored the association of differences in 5-gene expression and disease-specific survival, overall survival and progression-free interval in prostate cancer patients. Although high AMH expression was not significantly linked to low OS (overall survival) rate. Prostate cancer patients with low expression of SAA1 had poor Overall Survival ($p = 0.041$) (Fig. 4A), patients with elevated AMH expression levels had worse overall survival ($p = 0.127$) (Fig. 4B). And patients with OPRK1-low expression had poor disease-specific survival and overall survival ($p = 0.033$ and 0.022, respectively) (Fig. 4C,D); Progression-free interval and disease-specific survival ($p = 0.004$, 0.029, respectively) were obtained in patients with prostate cancer with low expression of IGF1 (Fig. 4E,F) [16].

3.5 The efficacy of prognostic identification was verified

To better understand how a model gene's expression affects clinical prognosis in prostate cancer, ROC curve analysis was used to verify its efficacy in differentiating different clinical outcomes. We first validated the diagnostic efficacy of a five-gene prognostic model for prostate cancer disease status as DEFA5 (AUC = 0.464), IGF1 (AUC = 0.636), SAA1 (AUC = 0.553), OPRK1 (AUC = 0.493), and AMH (AUC = 0.809), respectively (Fig. 5A). And then, we validated the efficacy of 5-gene prognostic models for the identification of Clinical variable outcomes of Alcohol history, Smoker, Lymphnode neck dissection, Radiation therapy, Age, Clinical stage, Histologic grade, Clinical T stage, pathologic stage, pathologic N stage, pathologic T stage, respectively (Fig. 5B–L). These results suggest that, for the assessment and anticipation of clinicopathological factors in prostate cancer, the 5-gene prognostic model may be a potential biomarker.

3.6 The prognostic model is associated with prostate cancer

To further explore the association of 5-gene prognostic models with prostate cancer, we explored their association with the expression of well-known molecular markers known to be associated with prostate cancer. We selected some reliable prostate cancer biomarkers for further analysis to explore whether the 5-gene prognostic model is associated with the molecular mechanisms of prostate cancer initiation and progression. It has been reported that transmembrane serine endopeptidase 2 (TMPRSS2) and ETS-related genes (ERG) frequently fuse during Principal component analysis (PCA) [17]. A mitochondrial and peroxisome enzyme, Alpha-methylacyl-coa racemase (AMACR), participates in fatty acid oxidation and intermediate products of bile acids [18]. The over-expression of AMACR on prostatic epithelial cells occurs in about 80% of prostate cancer cases, and the detection of AMACR by immunohistochemistry (IHC) helps to distinguish benign prostate cancer from prostate cancer [19]. At the same time, studies have reported that AMACR overexpression in prostate cells predicts poor prognosis (associated with a high Gleason score and high initial PSA levels) and an increased
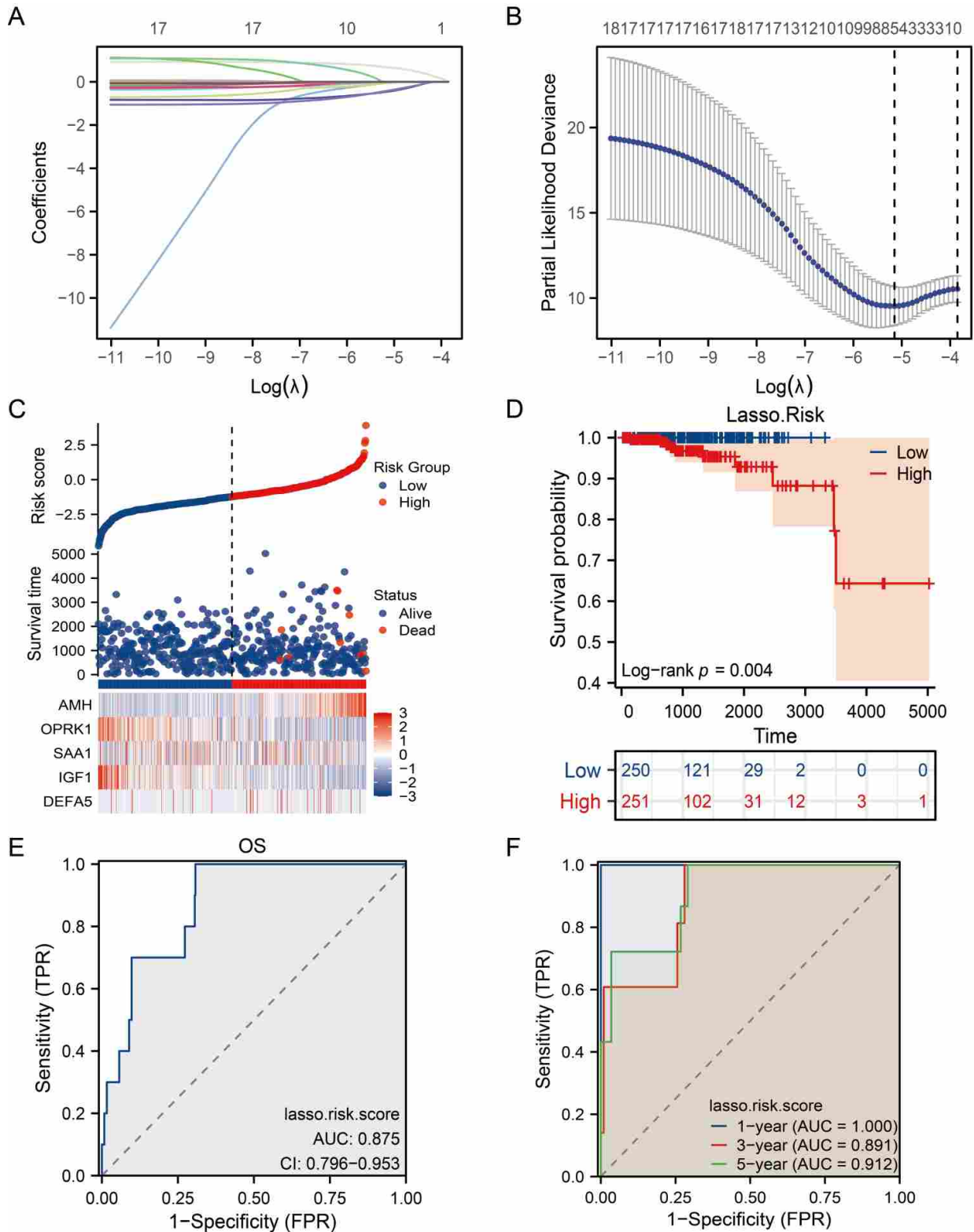
FIGURE 1. Lasso analysis and forest plot show multivariate Cox model results for 5 immune-related genes. (A) Cross validation of optimal parameter selection in LASSO model. (B) LASSO coefficient profiles of 18 prognostic immune-related genes; (C) The risk factor graph shows the distribution of risk scores (Top), the relationship between risk scores and survival time (middle), and the expression patterns of five immune-related genes in the high-and low-risk groups (bottom); (D) Kaplan-Meier curves of overall survival of PRAD patients in high- and low-risk score groups; (E) Receiver performance curve based on risk score; (F) Time-dependent receiver operating characteristic curves. AUC: area under the curve; TPR: True positive rate; FPR: False positive rate; OS: Overall survival; AMH: Anti-Mullerian Hormone; DEFA: Defensin Alpha; IGF: Insulin Like Growth Factor; OPRK: Opioid Receptor Kappa; SAA: Serum Amyloid A.

A

B

C
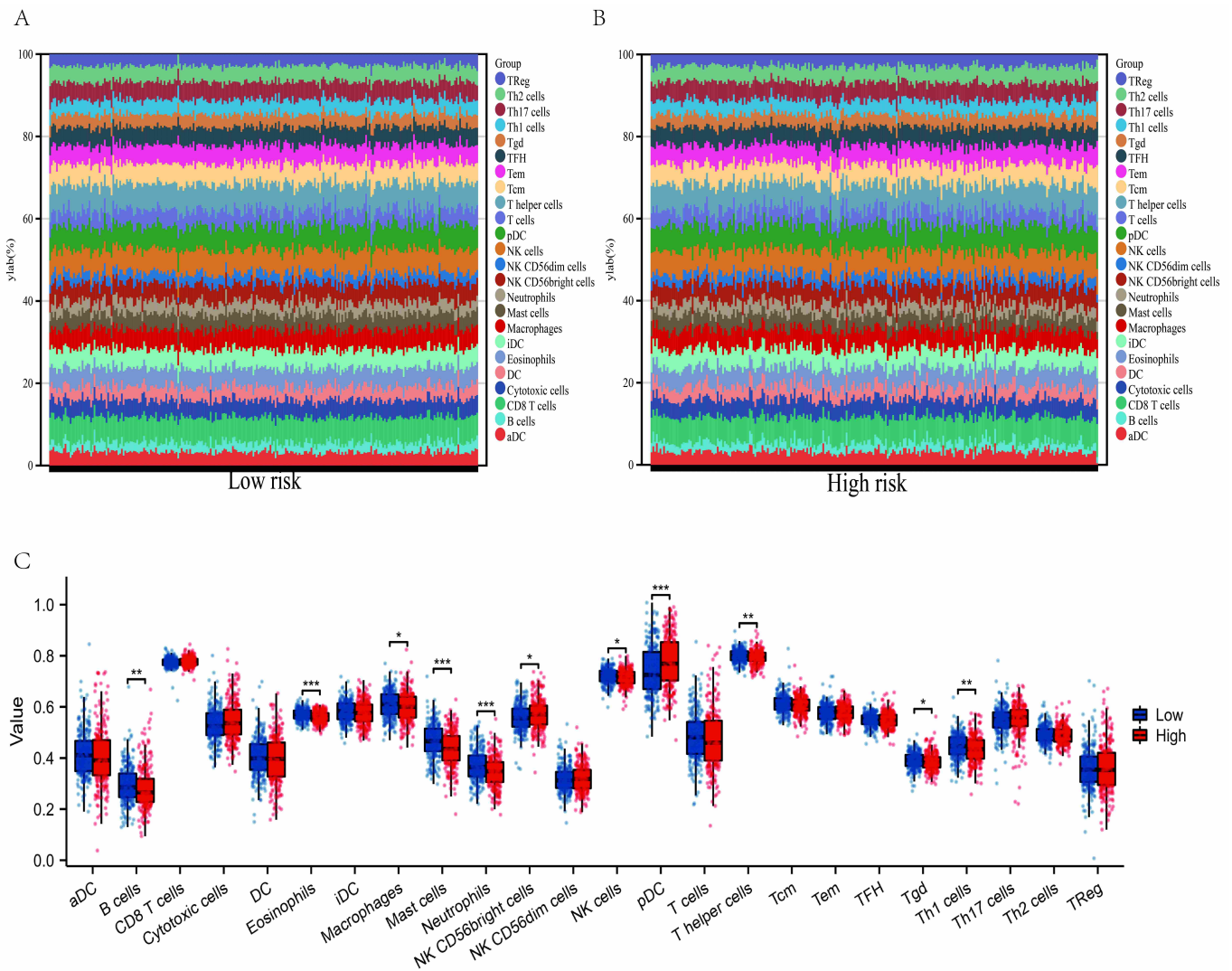
F I G U R E 2. Evaluation of immune infiltration. (A,B) Stacked bar graphs showing the proportion of infiltrating immune cells between the high-and low-risk groups. (C) Boxplot of the difference in immune cell infiltration between the high-and low-risk groups (Wilcoxon's test; *: $p < 0.05$; **: $p < 0.01$; ***: $p < 0.001$). Horizontal coordinates indicate the type of infiltrating immune cells, and the vertical axis indicates the proportion of infiltrating immune cells. Immune cell abbreviation: Th: Helper T lymphocytes; TR: regulatory T cell; NK: Natural killing cell; CD56: Neural Cell Adhesion Molecule 1; DC: Dendritic cell; PDC: plasmacytoid dendritic cell; TFH: Follicular helper T cells; Tgd: gamma delta T.

risk of bone metastasis. In addition, there have been reports linking several Solute Carrier Family 45 Member (SLC45A) family genes to prostate cancer [20–22]. As SLC45A3 (prostate cancer-associated protein 6/P501S/protein) is mainly expressed in the Gleason apparatus of prostate epithelial cells and is highly specific for prostate gland cells, it has been used to distinguish between other tumor types and metastatic prostate cancer [22, 23]. SLC45A3 may be expressed in PSA-negative prostate tumors, so the combined use of these markers may increase the sensitivity to identify prostate cancer metastases. SLC45A3 is weakly expressed in some aggressive tumors and is associated with increased Gleason score and risk of tumor recurrence. Overall findings revealed that in the 5-gene prognostic model, OPRK1 expression was positively linked to BRCA1 DNA Repair Associated (BRCA1), BRCA2 DNA Repair Associated (BRCA2), and AMACR (Fig. 6A,B,E). The positive correlation between OPRK1 expression and TMPRSS2 was significant, while the

negative correlation between SAA1, AMH and TMPRSS2 was significant (Fig. 6C). SAA1 was positively correlated with Hexokinase 3 (HK3), SLC45A1, SLC45A3, SLC45A4 (Fig. 6D,F–H).

3.7 Functional enrichment analysis

In addition, we summarised the differential genes between the low-risk and high-risk categories, followed by GO and KEGG enrichment analyses. Based on the results of the GO enrichment analysis (Fig. 7A–D & Table 3), the BP with significance were negative regulation of the reproductive process, ovulation cycle, oogenesis, interleukin-1 production and regulation of Interleukin-1 production, respectively. Cell component (CC) was enriched in transport vesicles, exocytic vesicles, cytoplasmic vesicle lumen, vesicle lumen and secretory granule lumen. Hormone activity, growth factor activity, insulin receptor binding, insulin-like growth factor receptor binding,
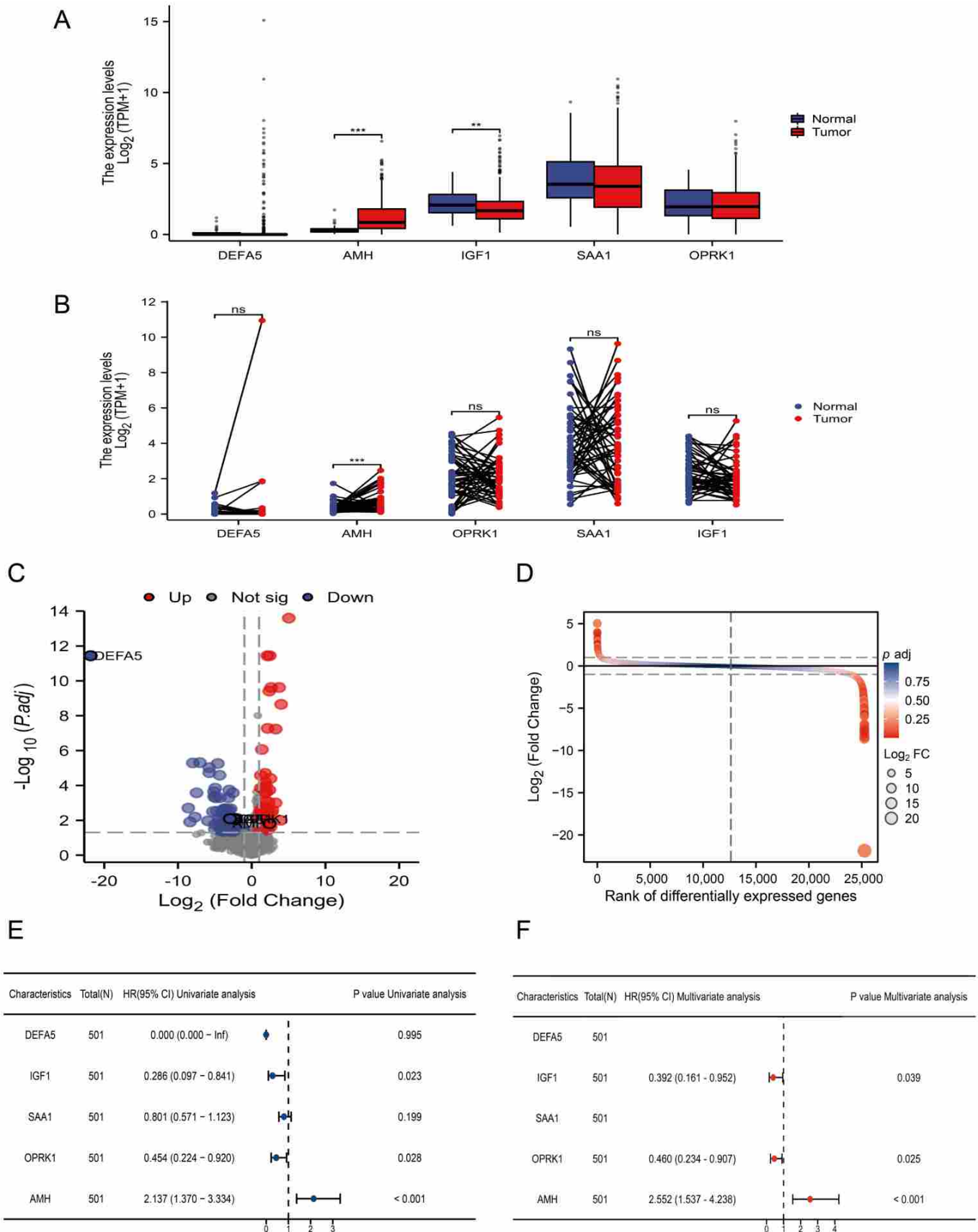
F I G U R E 3. Differential expression of prognostic DEIRGs in TCGA-PRAC. (A,B) The same difference was found in tumor tissues and normal samples. (C,D) Volcano plot and sequence plot showed the difference and significance of the five genes in the prognostic model based on the survival status of the patients. (E,F) Forest plot of 5 modifiers with prognostic value in univariate and multivariate Cox regression models. DEIRGs: Different expressed immune-related genes; TCGA: The Cancer Genome Atlas; PRAC: Prostate adenocarcinoma; AMH: Anti-Mullerian Hormone; DEFA5: Defensin Alpha 5; IGF1: Insulin Like Growth Factor 1; OPRK1: Opioid Receptor Kappa 1; SAA1: Serum Amyloid A1; GAPDH: Glyceraldehyde-3-Phosphate Dehydrogenase.

TABLE 2. Univariate and multivariate Cox regression analysis of predictive model molecules for prostate cancer prognosis.

Characteristics	Total	Univariate analysis		Multivariate analysis	
		HR (95% CI)	p	HR (95% CI)	p
Pathologic T stage	494		0.241		
T2	189	Reference			
T3	294	3.380 (0.631–18.091)	0.155		
T4	11	0.000 (0.000–Inf)	0.998		
Pathologic N stage	428		0.126		
N0	348	Reference			
N1	80	3.470 (0.767–15.695)	0.106		
Clinical T stage	407		0.023		
T1	177	Reference		Reference	
T2	175	0.850 (0.140–5.180)	0.860	0.000 (0.000–0.000)	<0.001
T3	53	6.808 (1.126–41.170)	0.037	2.907 (0.464–18.207)	0.254
T4	2	40.396 (3.510–464.903)	0.003	60195041998086.5000 (5776198188284.9502–627305878891122.0000)	<0.001
Clinical M stage	460		0.015		
M0	457	Reference		Reference	
M1	3	59.773 (6.563–544.434)	<0.001	0.000 (0.000 - Inf)	0.991
Primary therapy outcome	440		0.013		
PD	29	Reference		Reference	
SD	30	0.264 (0.030–2.370)	0.234	9.122 (0.803–103.612)	0.075
PR	40	0.343 (0.036–3.243)	0.350	1.727 (0.164–18.195)	0.649
CR	341	0.063 (0.011–0.350)	0.002	2.576 (0.275–24.138)	0.407
Race	486		0.727		
Asian	12	Reference			
Black or African American	58	6667525.5865 (0.000–Inf)	0.998		
White	416	9938185.1691 (0.000–Inf)	0.998		
Age	501		0.479		
≤60	225	Reference			
>60	276	1.578 (0.441–5.650)	0.484		
Residual tumor	470		0.157		
R0	316	Reference			
R1 & R2	154	2.587 (0.693–9.654)	0.157		
Zone of origin	277		0.466		
Central	4	Reference			
Peripheral	138	56367162.9214 (0.000–Inf)	1.000		

T A B L E 2. Continued.

Characteristics	Total	Univariate analysis		Multivariate analysis	
		HR (95% CI)	*p*	HR (95% CI)	*p*
Transition	8	0.795 (0.000–Inf)	1.000		
Multiple	127	94835394.6657 (0.000–Inf)	1.000		
PSA (ng/mL)	444		0.007		
<4	417	Reference		Reference	
≥4	27	10.528 (2.481–44.681)	0.001	9153146397117.3594 (967658373058.1670–86580234615534.2031)	<0.001
Gleason score	501		0.007		
6 & 7	294	Reference		Reference	
8 & 9 & 10	207	6.654 (1.371–32.298)	0.019	1721519.8672 (0.000–Inf)	0.990
IGF1	501		0.115		
Low	250	Reference			
High	251	0.306 (0.062–1.510)	0.146		
SAA1	501		0.035		
Low	250	Reference		Reference	
High	251	0.224 (0.047–1.068)	0.061	0.000 (0.000–0.000)	<0.001
OPRK1	501		0.013		
Low	250	Reference		Reference	
High	251	0.128 (0.016–1.020)	0.052	0.000 (0.000–Inf)	0.973
AMH	501		0.114		
Low	250	Reference			
High	251	3.219 (0.662–15.641)	0.147		

HR: Hazard ratio; CI: Confidence interval; CR: Complete response: PR: Partial response; SD: Stabilization disease; PD: Progressive disease; AMH: Anti-Mullerian Hormone; IGF1: Insulin Like Growth Factor 1; OPRK1: Opioid Receptor Kappa 1; SAA1: Serum Amyloid A1; PSA: prostate-specific antigen.

and transforming growth factor beta receptor binding were all enriched in MF. Furthermore, KEGG analysis revealed some immune-related pathways.

Subsequently, the 5 genes of the prognostic model were mapped in red letters on the KEGG pathway map. Pathway enrichment analysis suggested that the 5-gene prognostic model was enriched in aldosterone regulation, steroid production, long-term depression, longevity regulatory pathways, and Staphylococcus aureus infection, and the well-known Epidermal Growth Factor Receptor (EGFR), Hypoxia Inducible Factor 1 (HIF-1), The AMP-activated protein kinase (AMPK), and other signaling pathways, suggesting that a variety of cancer-related (Fig. 7E,F & Table 4). Fig. 8 shows the role of 5 genes involved in Prostate cancer, Long-term depression, Endocrine resistance, Transforming Growth Factor Beta (TGF-β) signaling pathway, and EGFR tyrosine kinase inhibitor resistance.

3.8 Gene set enrichment analysis based on a 5-gene prognostic model to predict differences between low and high-risk groups for prostate cancer

The potential mechanisms by which prognostic models regulate OS timing in PRAD patients need to be further explored. To find the possible signaling pathways involved in the prognostic model in the two risk groups, we performed GSEA (Fig. 9, **Supplementary Table 1**). The KEGG high-risk group was primarily enriched in Ribosome, Cell Cycle, Spliceosome, Ascorbate and Aldarate Metabolism, and Base Excision Repair, whereas the low-risk group was primarily enriched in Cardiac Muscle Contraction, Hypertrophic Cardiomyopathy HCM, Dilated Cardiomyopathy, Proximal Tubule Bicarbonate Reclamation, and Primary Immunodeficiency (Fig. 9A,B). In WikiPathways, high-risk groups were enriched in Striated Muscle Contraction Pathway, and Extrafollicular B Cell Acti-
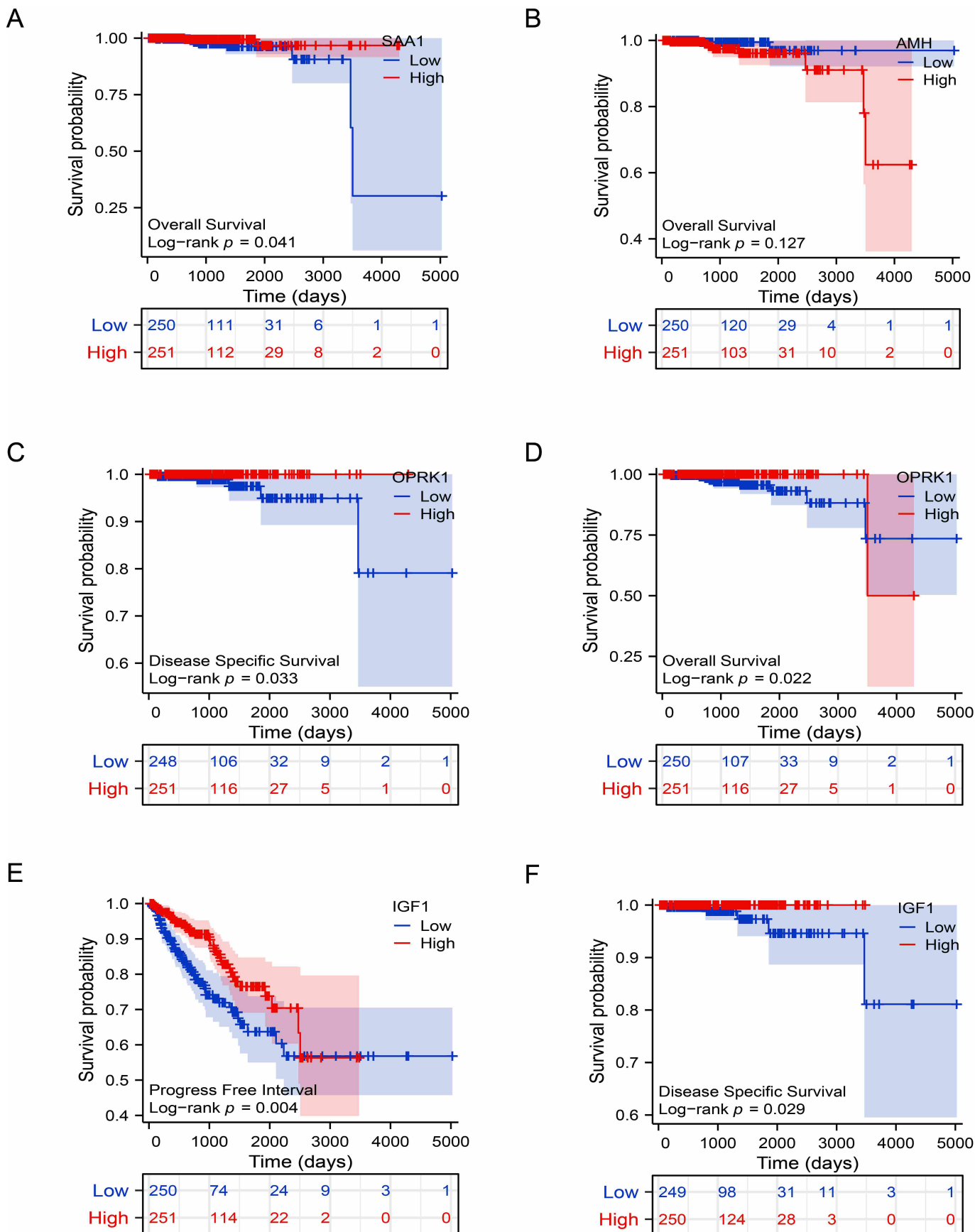
F I G U R E 4. The relationship between overall survival rate and gene expression of SAA1 (A), AMH (B), OPRK1 (D).
The relationship between disease-specific survival rate and gene expression of OPRK1 (C), IGF1 (F). The relationship between progression-free interval and gene expression of IGF1 (E). AMH: Anti-Mullerian Hormone; IGF1: Insulin Like Growth Factor 1; OPRK1: Opioid Receptor Kappa 1; SAA1: Serum Amyloid A1.
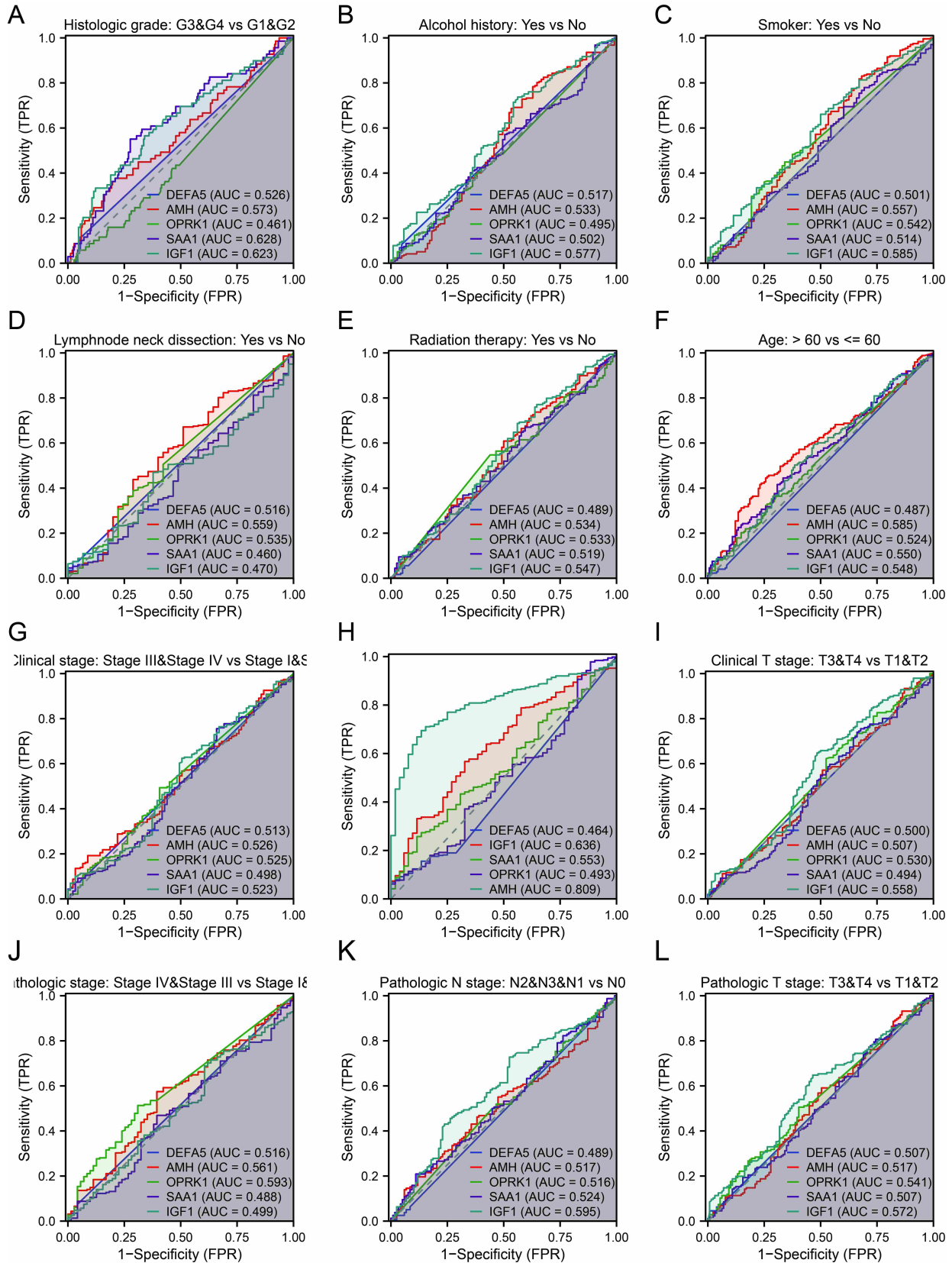
F I G U R E 5. ROC curves validate diagnostic efficacy. (A) The diagnostic efficacy of the 5-gene prognostic model for prostate cancer; (B–L) To verify the efficacy of the 5-gene prognostic model in the identification of Clinical variable outcomes of Alcohol history, Smoker, Lymphnode neck dissection, Radiation therapy, Age, Clinical stage, Histologic grade, Clinical t stage, Pathologic stage, Pathologic n stage, Pathologic T stage, respectively. AUC: area under the curve; AMH: Anti-Mullerian Hormone; IGF1: Insulin Like Growth Factor 1; OPRK1: Opioid Receptor Kappa 1; SAA1: Serum Amyloid A1. DEFA5: Defensin Alpha 5; TPR: True positive rate; FPR: False positive rate.
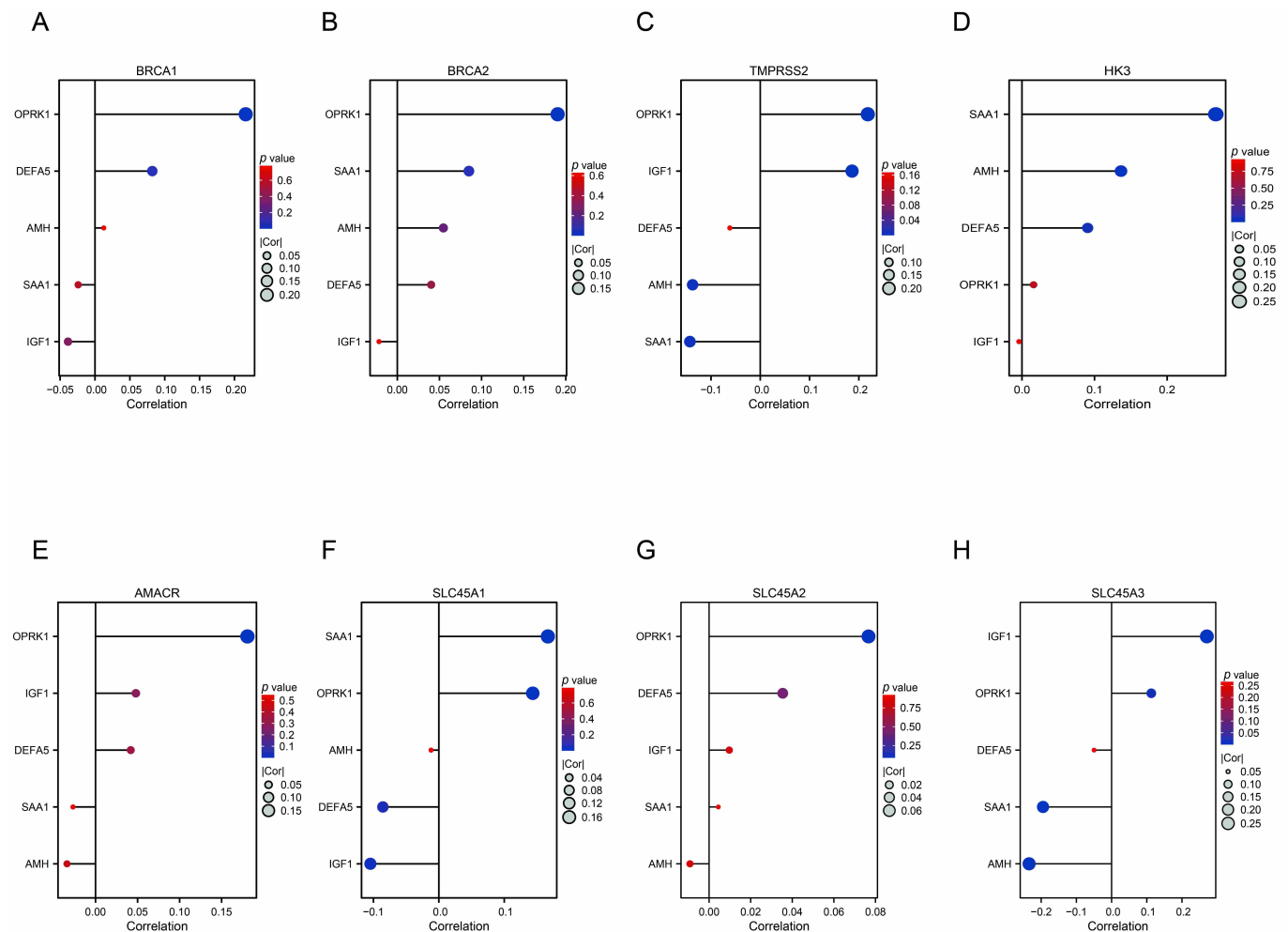
F I G U R E 6. Prognostic model is associated with prostate cancer. The overall results showed that the expression of OPRK1 in five prognostic model molecules was correlated with the expression of BRCA1, BRCA2 (A,B), TMPRSS2 (C), HK3 (D), AMACR (E), SLC45A1, SLC45A3, SLC45A4 (F–H) in lollipop graph, the size and color of the circle represent significance. BRCA1: BRCA1 DNA Repair Associated; AMH: Anti-Mullerian Hormone; IGF1: Insulin Like Growth Factor 1; OPRK1: Opioid Receptor Kappa 1; SAA1: Serum Amyloid A1; DEFA5: Defensin Alpha 5; HK3: Hexokinase 3; TMPRSS2: transmembrane serine endopeptidase 2; AMACR: Alpha-methylacyl-coa racemase.

vation by Sarscov2, Folate Metabolism, Selenium Micronutrient Network, and Complement System (Fig. 9C,D). The high-risk groups in the Reactome database were mostly enriched for striated muscle contraction, CD22-mediated B-cell receptor (BCR) regulation, clearance of heme in plasma, and creation of initial triggers for the complement system, such as C4 and C2 activators; The low-risk group was enriched in Striated Muscle Contraction, CD22 Mediated BCR Regulation, Scavenging of Heme from Plasma, spindle checkpoint and sister chromatid, of C 4 and C 2 creation Activators, Initial Triggering of Complement (Fig. 9E,F). In Persistent Identifier (PID), the high-risk group was enriched in Polo Like Kinase 1 (PLK1), ATR Serine/Threonine Kinase (ATR), Aurora B, Fanconi and Aurora a Pathway, while the low-risk group was enriched in NCADHERIN, INTEGRIN3, INTEGRIN2, Interleukin (IL42) pathways (Fig. 9G,H). Finally, the expression of hub gene was confirmed by PCR (Fig. 10).

4. Discussion

Overall, we analyzed DEIRGs associated with PRAD prognosis by LASSO regression, with predicted prognostic models including DEFA5, IGF1, SAA1, OPRK1 and AMH. During cancer development, t-cell infiltration is impaired, antigen regulation is disrupted, and expression levels of immune checkpoints and their ligands are elevated [24]. Hence, patients may not benefit greatly from ICI treatment when immune checkpoints are not the only rate-limiting step [25]. Patients in the current study who had low risk scores had a higher level of immune checkpoint molecules. Indirectly, the rise in immune checkpoint levels, including PD-1 and Cytotoxic T-Lymphocyte Associated Protein 4 (CTLA-4), in the low-risk score group suggests pre-existing t-cell activation. Patients with low-risk scores may therefore be more sensitive to ICI treatment [26].

Although we elucidated the role of the 5-gene prognostic model in predicting prognosis and verified the expression levels of DEFA5, IGF1, SAA1, OPRK1 and AMH in tumor
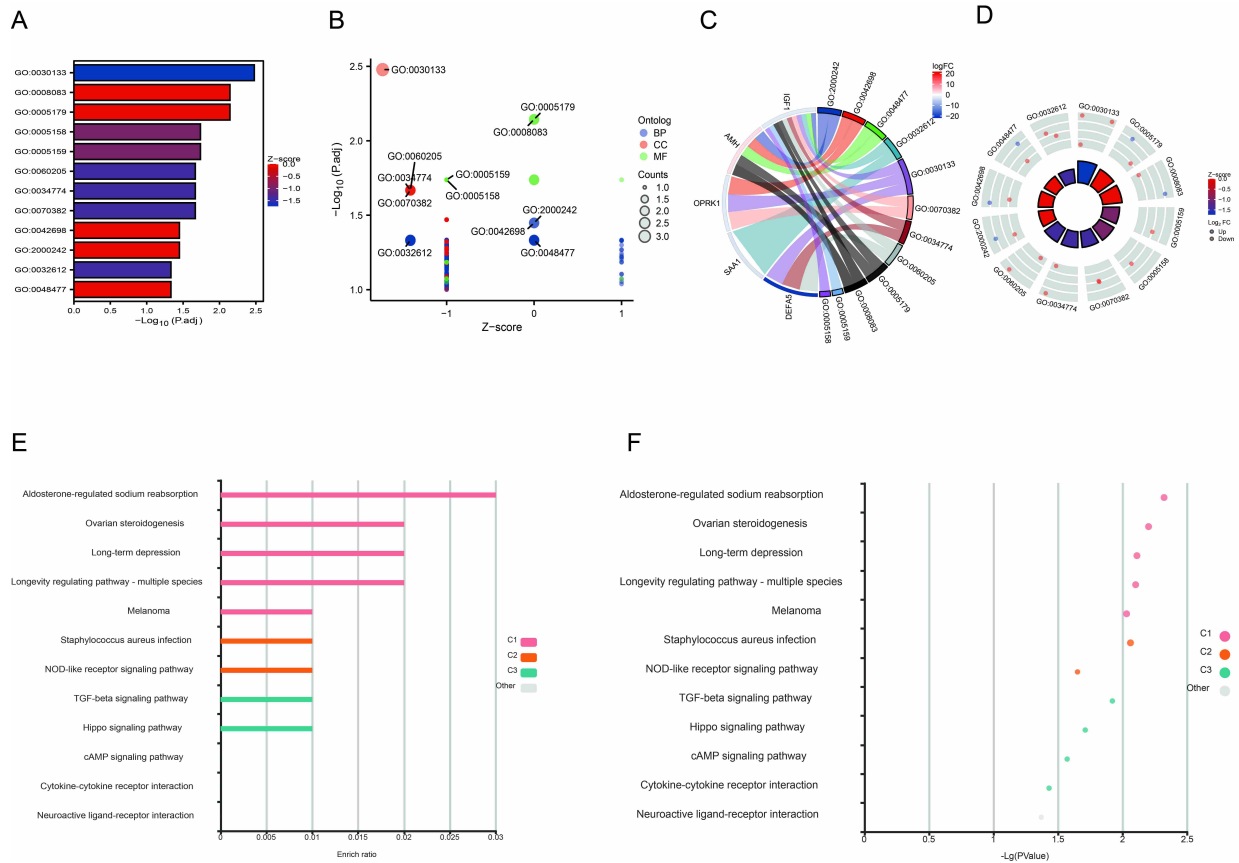
FIGURE 7. GO and KEGG enrichment analysis of 5-gene prognostic model molecules. (A–D) GO enrichment analysis bar graph, bubble graph, chord graph and cycle graph; (E,F) Kobas database was used to analyze the KEGG pathway enrichment results of the 5-gene prognostic model. GO: Gene Ontology; BP: Biological process; CC: Cell component; MF: Molecular function; AMH: Anti-Mullerian Hormone; IGF1: Insulin Like Growth Factor 1; OPRK1: Opioid Receptor Kappa 1; SAA1: Serum Amyloid A1; DEFA5: Defensin Alpha 5; TGF-β: Transforming Growth Factor Beta; cAMP: Cyclic adenosine monophosphate.

TABLE 3. GO enrichment results of prognostic model.

Ontology	ID	Description	adj.p
BP	GO: 2000242	negative regulation of reproductive process	0.0356
BP	GO: 0042698	ovulation cycle	0.0356
BP	GO: 0048477	oogenesis	0.0465
BP	GO: 0032612	interleukin-1 production	0.0465
BP	GO: 0032652	regulation of interleukin-1 production	0.0465
CC	GO: 0030133	transport vesicle	0.0033
CC	GO: 0070382	exocytic vesicle	0.0215
CC	GO: 0034774	secretory granule lumen	0.0215
CC	GO: 0060205	cytoplasmic vesicle lumen	0.0215
CC	GO: 0031983	vesicle lumen	0.0215
MF	GO: 0005179	hormone activity	0.0072
MF	GO: 0008083	growth factor activity	0.0072
MF	GO: 0005159	insulin-like growth factor receptor binding	0.0183
MF	GO: 0005158	insulin receptor binding	0.0183
MF	GO: 0005160	transforming growth factor beta receptor binding	0.0183

GO: Gene Ontology; BP: Biological process; CC: Cell component; MF: Molecular function.

T A B L E 4. KEGG enrichment results of prognostic model.

Term	ID	Background number	adj.p
Aldosterone-regulated sodium reabsorption	hsa04960	37	0.004832
Ovarian steroidogenesis	hsa04913	49	0.006354
Long-term depression	hsa04730	60	0.007747
Longevity regulating pathway-multiple species	hsa04213	62	0.008000
Staphylococcus aureus infection	hsa05150	68	0.008760
p53 signaling pathway	hsa04115	72	0.009266
Melanoma	hsa05218	72	0.009266
Glioma	hsa05214	75	0.009645
EGFR tyrosine kinase inhibitor resistance	hsa01521	79	0.010150
Longevity regulating pathway	hsa04211	89	0.011413
Hypertrophic cardiomyopathy (HCM)	hsa05410	90	0.011540
TGF-beta signaling pathway	hsa04350	94	0.012044
Dilated cardiomyopathy (DCM)	hsa05414	96	0.012297
Prostate cancer	hsa05215	97	0.012423
Endocrine resistance	hsa01522	98	0.012549
Progesterone-mediated oocyte maturation	hsa04914	99	0.012675
Inflammatory mediator regulation of TRP channels	hsa04750	100	0.012801
HIF-1 signaling pathway	hsa04066	109	0.013935
AMPK signaling pathway	hsa04152	120	0.015320

EGFR: Epidermal Growth Factor Receptor; TGF-β: Transforming Growth Factor Beta; TPR: True positive rate; HIF-1: Hypoxia Inducible Factor 1; AMPK: AMP-activated protein kinase.

tissues by proteomics, there are still some limitations, to be further explored. To explore the characteristic function of prostate cancer, AMH and OPRK1 were found to be the key genes affecting Tumor microenvironment (TMB) and potential targets for immunotherapy. It was suggested that higher expression of AMH was beneficial to PCA progression, and patients' OS was worse when the OPRK1 level was lower, along with a higher recurrence rate in the early stage of PCA than those with high expression of OPRK1 [23, 27]. The onset and progression of prostate cancer may be influenced by decreased circulation levels of the testis-derived TGF-family peptide hormone, anti-mullerian hormone (AMH) [28]. In a study of 1000 patients, the overall risk of prostate cancer has been demonstrated to be correlated with prediagnostic serum AMH levels [29]. Physiological concentrations of endogenous AMH increased the viability of cancer cells [30]. Furthermore, serum amyloid A1 (SAA1) is an inflammatory high-density lipoprotein. It is also regarded as a prognostic indicator and a predictor of cancer risk [31]. It is crucial for fatty acid oxidation (FAO), Association of Tennis Professiona (ATP) and cell growth in prostate cancer tissues, which are induced by the loss of the cancer biomarkers SUN2 [32, 33]. The inhibitory effect of the IGF1/Signal Transducer and Activator of Transcription 3 (STAT3) pathway on the invasion of prostate cancer is well known [34]. Correlations between IGF1 and Wnt/β-catenin signaling have also been found in human prostate cancer samples [35]. Single-cell transcriptomic analysis has shown that AR activation enhances the

mecasermin signaling pathway (IGF1) and initiates oncogenic transformation [36]. Elevated IGF1 signaling further accumulates the Wnt/β-catenin pathway in transformed cells to promote prostate tumor development [37]. The detection rate of DEFA5 in cancer was significantly higher in patients. In addition to the role of defensins in the innate immune system, which is associated with antimicrobial and immune signaling activities, the significance of α-defensin 5 (DEFA5) in the onset and progression of gastric cancer is being discussed in an increasing number of studies [3, 38]. A study showed mechanistically how DEFA5 binds to Body Mass Index (BMI) directly, then decreases its binding at the Cyclin Dependent Kinase Inhibitor 2A (CDKN2A) locus, and upregulates the expression of the cyclin-dependent kinase inhibitors p16 and p19 to inhibit stomach cancer [1, 2].

To further improve the reliability and persuasiveness of guiding clinical strategic decisions, we incorporated expression profiles and survival data from TCGA prostate cancer during the analysis. In addition, it was shown that several specific DEIRGs with remarkable variations in variable risk factors were linked to the advancement of prostate cancer and patient prognosis. More importantly, these DEIRGs, as molecular biomarkers, have an important role in predicting and evaluating survival outcomes in prostate cancer.

Despite some positive results, there are still some problems. First, this immune signature is built on a common data set. Predictive power needs to be further tested in Randomized controlled trials. First, we did not combine metabolomics

A

B

C

D

E

F

F I G U R E 8. KOBAS database was used to analyze the KEGG pathway of 5-gene prognostic model. (A) Prostate cancer, (B) Long-term depression, (C) Endocrine resistance, (D) Epidermal Growth Factor Receptor (EGFR) tyrosine kinase inhibitor resistance, (E) Transforming Growth Factor Beta (TGF-β) signaling pathway, (F) p53 signaling pathway.
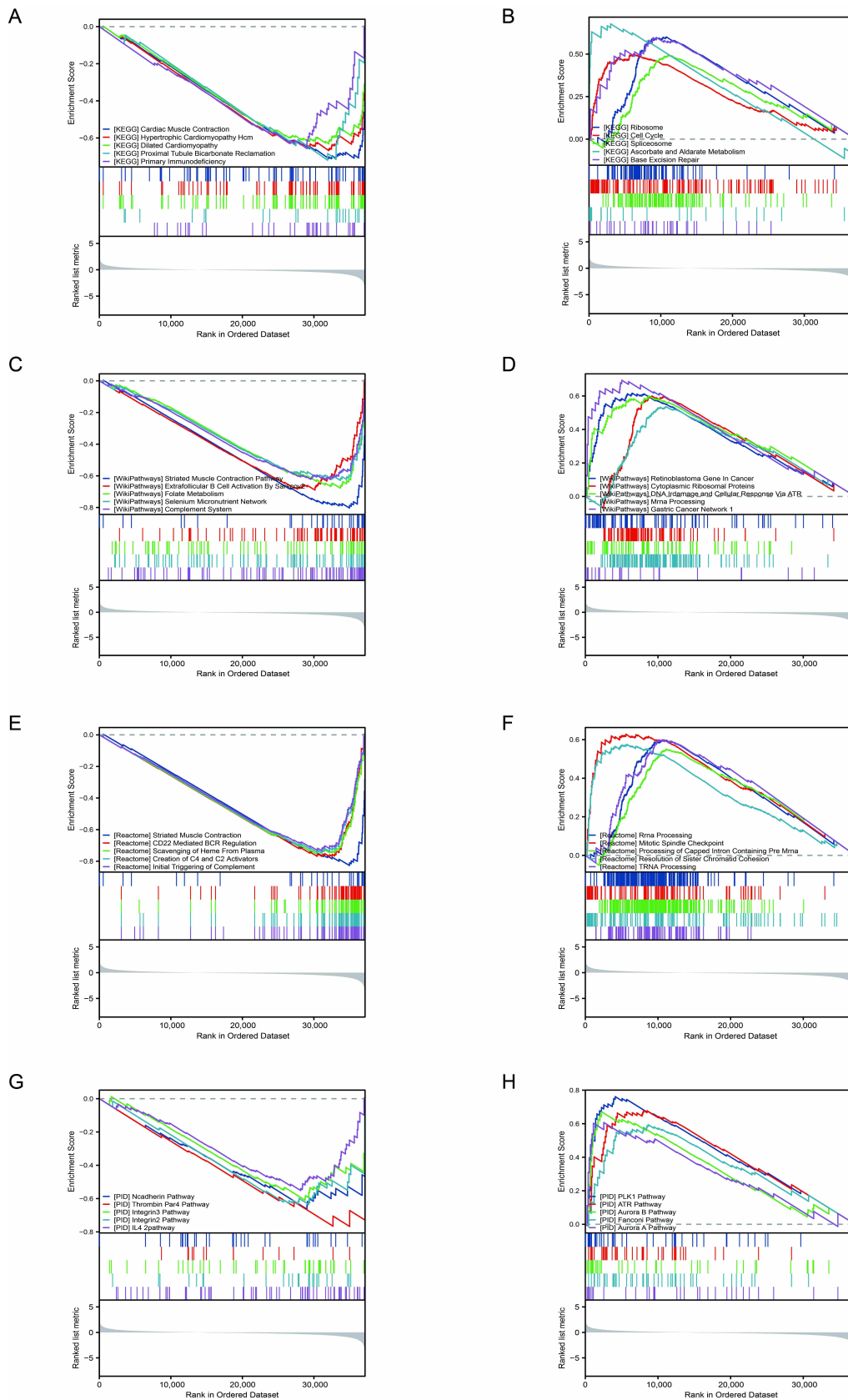
FIGURE 9. Gene set enrichment analysis based on a 5-gene prognostic model to predict differences between high-and low-risk groups for prostate cancer. Significant enrichment entries were included in the REACTOME (A,B), WP (C), PID (D), Kegg (E) and BIOCARTA (F) databases, respectively. KEGG: Kyoto Encyclopedia of Genes and Genomes; PID: Persistent Identifier. ATR: Serine/Threonine Kinase; CD56: Neural Cell Adhesion Molecule 1; PID: Persistent Identifier; PLK1: Polo Like Kinase 1; IL42: Interleukin; BCR: B-cell receptor.
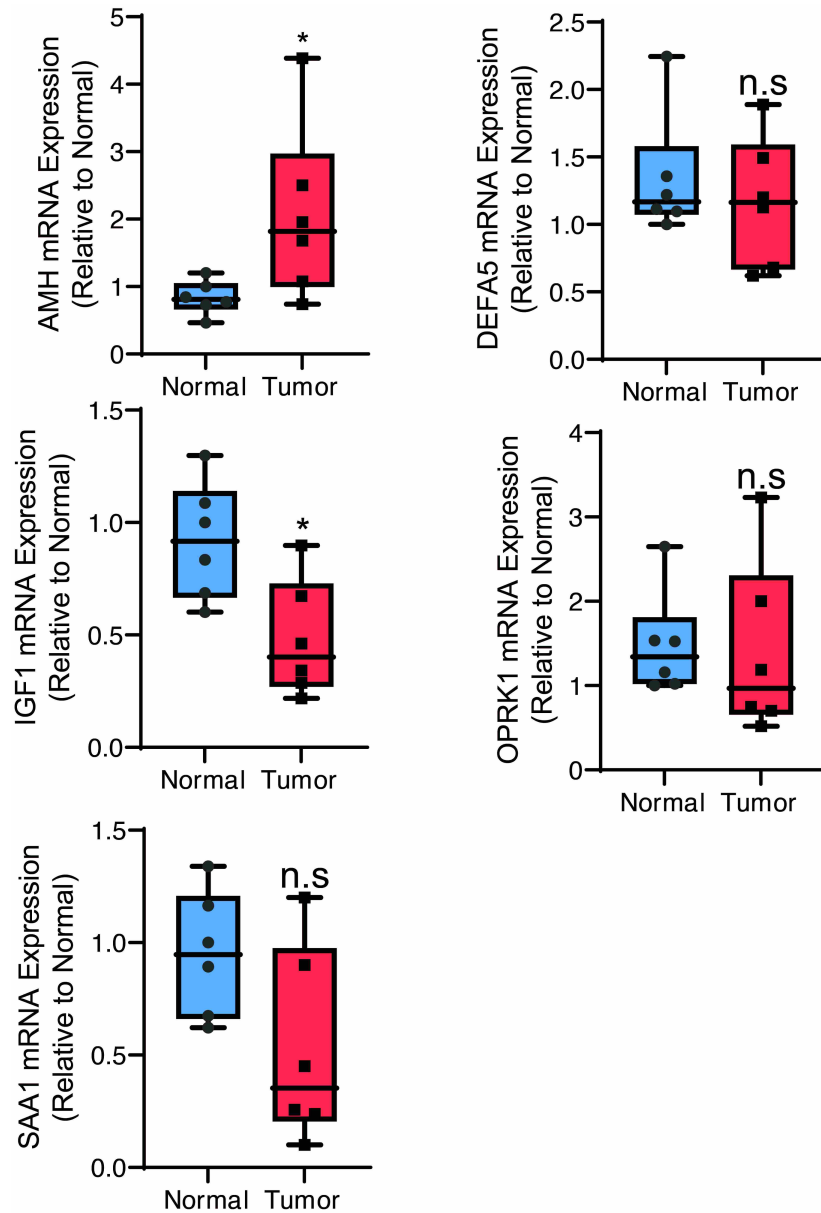
F I G U R E 1 0. The gene expression of hub genes by PCR. AMH: Anti-Mullerian Hormone; DEFA5: Defensin Alpha 5; IGF1: Insulin Like Growth Factor 1; OPRK1: Opioid Receptor Kappa 1; SAA1: Serum Amyloid A1.

with immunogenomics testing. In addition, the practical value of our prognostic gene model for prostate cancer needs to be further validated. To sum up, we comprehensively analyzed and validated 5-gene prognostic models to predict the clinical prognosis of prostate cancer. The findings will help to establish a reliable and referential risk assessment model and provide new insights into immune-related research and treatment strategies.

5. Conclusions

In this study, we constructed prognostic immunoprofiles based on the TCGA-PRAD dataset and tested their predictive power on both total and internal datasets. There was a significant difference in tumor infiltrating lymphocytes between high-risk and low-risk groups, and an immune marker composed of five immune-related genes was an independent predictor of PRAD patients. Patients in the low-risk category had better overall

survival and greater infiltration of immune cells in the tumor microenvironment, which is highly correlated with clinical outcomes but requires prospective validation.

AVAILABILITY OF DATA AND MATERIALS

The data are contained within this article and supplementary material.

AUTHOR CONTRIBUTIONS

ETHICS APPROVAL AND CONSENT TO PARTICIPATE

Not applicable.

ACKNOWLEDGMENT

Not applicable.

FUNDING

CONFLICT OF INTEREST

The authors declare no conflict of interest.

SUPPLEMENTARY MATERIAL

Supplementary material associated with this article can be found, in the online version, at https://oss.jomh.org/files/article/1730114122003955712/attachment/Supplementary%20material.docx.

REFERENCES

[1] Jiang T, Guo J, Hu Z, Zhao M, Gu Z, Miao S. Identification of potential prostate cancer-related pseudogenes based on competitive endogenous RNA network hypothesis. Medical Science Monitor. 2018; 24: 4213–4239.

[2] Wu Z, Ding Z, Cheng B, Cui Z. The inhibitory effect of human DEFA5 in growth of gastric cancer by targeting BMI1. Cancer Science. 2021; 112: 1075–1083.

[3] Ding Y, Wu H, Warden C, Steele L, Liu X, Iterson MV, et al. Gene expression differences in prostate cancers between young and old men. PLOS Genetics. 2016; 12: e1006477.

[4] Li B, Severson E, Pignon J, Zhao H, Li T, Novak J, et al. Comprehensive analyses of tumor immunity: implications for cancer immunotherapy. Genome Biology. 2016; 17: 174.

[5] Zhang B, Zhou YL, Chen X, Wang Z, Wang Q, Ju F, et al. Efficacy and safety of CTLA-4 inhibitors combined with PD-1 inhibitors or chemotherapy in patients with advanced melanoma. International Immunopharmacology. 2019; 68: 131–136.

[6] Ogata H, Goto S, Sato K, Fujibuchi W, Bono H, Kanehisa M. KEGG: Kyoto encyclopedia of genes and genomes. Nucleic Acids Research. 1999; 27: 29–34.

[7] Walter W, Sánchez-Cabo F, Ricote M. GOplot: an R package for visually combining expression data with functional analysis. Bioinformatics. 2015; 31: 2912–2914.

[8] Chkaiban L, Tosi L, Parekkadan B. Assembly of long-adapter single-strand oligonucleotide (LASSO) probes for massively parallel capture of kilobase size DNA targets. Current Protocols. 2021; 1: e278.

[9] Nahm FS. Receiver operating characteristic curve: overview and practical use for clinicians. Korean Journal of Anesthesiology. 2022; 75: 25–36.

[10] Jin X, Xie H, Liu X, Shen Q, Wang Z, Hao H, et al. RELL1, a novel oncogene, accelerates tumor progression and regulates immune infiltrates in glioma. International Immunopharmacology. 2020; 87: 106707.

[11] Kim TJ, Koo KC. Current status and future perspectives of checkpoint inhibitor immunotherapy for prostate cancer: a comprehensive review. International Journal of Molecular Sciences. 2020; 21: 5484.

[12] Craven KE, Gökmen-Polar Y, Badve SS. CIBERSORT analysis of TCGA and METABRIC identifies subgroups with better outcomes in triple negative breast cancer. Scientific Reports. 2021; 11: 4691.

[13] Heagerty PJ, Zheng Y. Survival model predictive accuracy and ROC curves. Biometrics. 2005; 61: 92–105.

[14] Lu Z, Chen Y, Chen S, Zhu X, Wang C, Wang Z, et al. Comprehensive prognostic analysis of immune implication value and oxidative stress significance of NECAP2 in low-grade glioma. Oxidative Medicine and Cellular Longevity. 2022; 2022: 1–39.

[15] Ren S, Wang W, Shen H, Zhang C, Hao H, Sun M, et al. Development and validation of a clinical prognostic model based on immune-related genes expressed in clear cell renal cell carcinoma. Frontiers in Oncology. 2020; 10: 1496.

[16] Ge X, Wang Z, Jiang R, Ren S, Wang W, Wu B, et al. SCAMP4 is a novel prognostic marker and correlated with the tumor progression and immune infiltration in glioma. The International Journal of Biochemistry & Cell Biology. 2021; 139: 106054.

[17] Khosh Kish E, Choudhry M, Gamallat Y, Buharideen SM, D D, Bismar TA. The expression of proto-oncogene ETS-related gene (ERG) plays a central role in the oncogenic mechanism involved in the development and progression of prostate cancer. International Journal of Molecular Sciences. 2022; 23: 4772.

[18] Schöpf B, Weissensteiner H, Schäfer G, Fazzini F, Charoentong P, Naschberger A, et al. OXPHOS remodeling in high-grade prostate cancer involves mtDNA mutations and increased succinate oxidation. Nature Communications. 2020; 11: 1487.

[19] Mehra R, Kumar-Sinha C, Shankar S, Lonigro RJ, Jing X, Philips NE, et al. Characterization of bone metastases from rapid autopsies of prostate cancer patients. Clinical Cancer Research. 2011; 17: 3924–3932.

[20] Makino Y, Kamiyama Y, Brown JB, Tanaka T, Murakami R, Teramoto Y, et al. Comprehensive genomics in androgen receptor-dependent castration-resistant prostate cancer identifies an adaptation pathway mediated by opioid receptor kappa 1. Communications Biology. 2022; 5: 299.

[21] Shtivelman E, Beer TM, Evans CP. Molecular pathways and targets in prostate cancer. Oncotarget. 2014; 5: 7217–7259.

[22] Cochran M, East K, Greve V, Kelly M, Kelley W, Moore T, et al. A study of elective genome sequencing and pharmacogenetic testing in an unselected population. Molecular Genetics & Genomic Medicine. 2021; 9: e1766.

[23] Hernández-Llodrà S, Juanpere N, de Muga S, Lorenzo M, Gil J, Font-Tello A, et al. ERG overexpression plus SLC45A3 (prostein) and PTEN expression loss: strong association of the triple hit phenotype with an aggressive pathway of prostate cancer progression. Oncotarget. 2017; 8: 74106–74118.

[24] Mariathasan S, Turley SJ, Nickles D, Castiglioni A, Yuen K, Wang Y, et al. TGFβ attenuates tumour response to PD-L1 blockade by contributing to exclusion of T cells. Nature. 2018; 554: 544–548.

[25] Brackenier C, Kinget L, Cappuyns S, Verslype C, Beuselinck B, Dekervel J. Unraveling the synergy between atezolizumab and bevacizumab for the treatment of hepatocellular carcinoma. Cancers. 2023; 15: 348.

[26] Chen DS, Mellman I. Oncology meets immunology: the cancer-immunity cycle. Immunity. 2013; 39: 1–10.

[27] Wang L, Yao Y, Xu C, Wang X, Wu D, Hong Z. Exploration of the tumor mutational burden as a prognostic biomarker and related hub gene identification in prostate cancer. Technology in Cancer Research & Treatment. 2021; 20: 15330338211052154.

[28] Lin D, Ettinger SL, Qu S, Xue H, Nabavi N, Chuen Choi SY, et al. Metabolic heterogeneity signature of primary treatment-naïve prostate cancer. Oncotarget. 2017; 8: 25928–25941.

[29] Sklavos MM, Zhou CK, Pinto LA, Cook MB. Prediagnostic circulating anti-Müllerian hormone concentrations are not associated with prostate cancer risk. Cancer Epidemiology, Biomarkers & Prevention. 2014; 23: 2597–2602.

[30] Chauvin M, Garambois V, Colombo PE, Chentouf M, Gros L, Brouillet JP, et al. Anti-Müllerian hormone (AMH) autocrine signaling promotes survival and proliferation of ovarian cancer cells. Scientific Reports. 2021; 11: 2231.

[31] Cao K, Jiang X, Wang B, Ni Z, Chen Y. SAA1 Expression as a potential prognostic marker of the tumor microenvironment in glioblastoma. Frontiers in Neurology. 2022; 13: 905561.

[32] Yajun C, Chen Y, Xiaosa L, Xiao W, Jia C, Zhong W, et al. Loss of Sun2 promotes the progression of prostate cancer by regulating fatty acid oxidation. Oncotarget. 2017; 8: 89620–89630.

[33] Zhang H, Xu Y, Deng G, Yuan F, Tan Y, Gao L, *et al*. SAA1 knockdown promotes the apoptosis of glioblastoma cells *via* downregulation of AKT signaling. Journal of Cancer. 2021; 12: 2756–2767.

[34] Ma JB, Bai JY, Zhang HB, Jia J, Shi Q, Yang C, *et al*. KLF5 inhibits STAT3 activity and tumor metastasis in prostate cancer by suppressing IGF1 transcription cooperatively with HDAC1. Cell Death & Disease. 2020; 11: 466.

[35] Samaržija I. Post-translational modifications that drive prostate cancer progression. Biomolecules. 2021; 11: 247.

[36] Mirzaei S, Paskeh MDA, Okina E, Gholami MH, Hushmandi K, Hashemi M, *et al*. Molecular landscape of LncRNAs in prostate cancer: a focus on pathways and therapeutic targets for intervention. Journal of Experimental & Clinical Cancer Research. 2022; 41: 214.

[37] Kim WK, Olson AW, Mi J, Wang J, Lee DH, Le V, *et al*. Aberrant androgen action in prostatic progenitor cells induces oncogenesis and tumor development through IGF1 and Wnt axes. Nature Communications. 2022; 13: 4364.

[38] Born J, Hendricks A, Hauser C, Egberts JH, Becker T, Röder C, *et al*. Detection of marker associated with CTC in colorectal cancer in mononuclear cells of patients with benign inflammatory intestinal diseases. Cancers. 2021; 14: 47.